



## Improved Pervaporation Performance of 13X Zeolite Filled Chitosan Membranes

H. Sudhakar<sup>1</sup>, Y. Maruthi<sup>1</sup>, U. Sajan Kumarji Rao<sup>2</sup>, C. Venkata Prasad<sup>4</sup>, M.C.S.Subha<sup>3</sup>,  
S. Sridhar<sup>2</sup>, K. Chowdoji Rao<sup>1\*</sup>

<sup>1</sup>Department of Polymer Science & Technology, Sri Krishnadevaraya University, Anantapuramu, India.

<sup>2</sup>Membrane Separations Group, Chemical Engineering Division, Indian Institute of Chemical Technology, Hyderabad, India.

<sup>3</sup>Department of Chemistry, Sri Krishnadevaraya University, Anantapuramu, India.

<sup>4</sup>Central Power Research Institute, Prof. Sir. C.V. Raman Road, Sadhashiva Nagar, Bengaluru, India.

Received 29<sup>th</sup> October 2013; Revised 10<sup>th</sup> November 2013; Accepted 24<sup>th</sup> November 2013.

### ABSTRACT

Novel polymeric membranes were prepared by incorporating the 13X zeolite into chitosan by solution casting method. The resulting composite membranes were characterized by Fourier transform infrared spectroscopy, X-ray diffraction, scanning electron microscopy, thermogravimetric analysis and differential scanning calorimetry. The results indicate that the chitosan membranes showed preferential permeation to water for 5-40% water in feed compositions. The experimental results further revealed that both the flux and selectivity increased simultaneously with increasing zeolite content in the membrane when compared to the unmodified chitosan membranes. This was explained on the basis of enhancement of hydrophilicity, selective adsorption and molecular sieving action by the creation of pores due to zeolites presence in the membrane matrix. The membrane containing 30 wt. % of zeolite shows the highest separation selectivity of 1620 at 30 °C for 5 mass% of water in the feed.

**Keywords:** Pervaporation, Chitosan, Isopropanol-Water, Azeotrope, Zeolite, Mixed Matrix Membrane.

### 1. INTRODUCTION

Chemical separation by pervaporation (PV) technique is one of the most popular areas of current membrane research [1]. PV is a combination of preferential permeation followed by evaporation. On one side of the membrane the preferentially sorbed fluid is in the liquid state, and it is withdrawn through the membrane as preferentially sorbed vapor by applying a vacuum on the other side of the membrane [2]. The possible application areas for PV separation in industry are numerous, including separation of azeotropic mixtures [3-4], separation of mixture of organic liquids [5-6], dehydration of organic solvents [7-8] and continuous removal of one of the products of reaction from a bioreactor [9]. Separation of the liquids is governed by the chemical nature of the permeating species as well as that of the membrane material, and the morphology of the membrane itself together with the experimental conditions of process operation [10-11]. Purification of organic solvents such as isopropanol (IPA), containing a small amount of water is of vital significance in the area of organic synthesis. Isopropanol is one of the important solvents used on a large scale in chemical industry as well as in pharmaceutical laboratories. Further, it has also been used in semi-

-conductor and liquid crystal display industries as a water-removing agent [12-13]. IPA and water form an azeotropic mixture at a concentration of 87.5 wt% (IPA) [14] and hence, the separation of these mixtures by conventional methods such as solvent extraction and rotavapor or by distillation could prove uneconomical. Several membrane materials have been modified recently for the selective separation of water from aqueous mixtures of isopropanol [15]. However, the membranes employed in such separation studies often yield compromised results of flux and selectivity due to trade-off phenomenon existing between the flux and separation factor in PV process.

Chitosan [poly-(1→4)-d-glucosamine] is a partially deacetylated from chitin [poly-(1→4)-N-acetyl-d-glucosamine], which is found in a wide range of natural sources like crab, lobster and shrimp shells. Recently many investigators [16-18] have been extensively used chitosan as a pervaporation membrane material due to its extremely high affinity towards water, good film forming properties, functional groups that can be easily modified apart from its good mechanical and chemical stability. However, the performance of

\*Corresponding Author:

E-mail address: chowdojirao@gmail.com

pure chitosan membrane is not satisfactory at higher concentration of water due to a large free volume available between the molecular chains [19]. Due to its high hydrophilicity, chitosan is a good material for preparation of pervaporation membranes. Chitosan membranes can be prepared by dry process, in which chitosan/acid/water solution is evaporated to form dense membranes. However, such membranes cannot be directly used in pervaporation because the membrane would re-dissolve when being in contact with aqueous solution, an effect caused by the residual acid in the membrane. Even after the removal of the residual acid, the membrane would still be not stable when being applied to the pervaporation process, because of the swelling effect caused by the aqueous solution in the feed. Thus, a cross-linking process is usually required. Sulfuric acid, aldehyde, and dialdehyde are common cross linkers. After cross-linking, although the stability and perm selectivity are improved, the permeation flux is low, which limits the application of chitosan membranes to pervaporation. Therefore, in the present work, a different approach is used: inorganic particles are embedded into the chitosan membrane to reduce swelling and thus to improve membrane selectivity. Alternatively, incorporation of a high selective zeolite into membrane matrix can also be effective. Since zeolites have a high surface area and uniform pore size distribution, and hence these have been used widely in chemical and physical processes such as shape selective catalysis and separation media [20].

The zeolite-incorporated polymer membranes have received much attention recently in gas and pervaporation separation studies. The incorporation of such zeolites or porous fillers in dense membranes can improve the separation performance of PV membranes [21-24] due to the combined effects of molecular sieving action, selective adsorption and difference in diffusion rates. In addition, zeolites have high mechanical strength, good thermal and chemical stability and thus, the membranes incorporated with these zeolites, can be used over a wide range of operating conditions.

In the present study, 13X zeolite (particle size: 2.67  $\mu\text{m}$ , pore size: 7.4  $\text{Å}$ , Si/Al ratio: 1.43), were incorporated into the chitosan and pervaporation studies through IPA-water mixtures have been carried out and the results were discussed in terms of PV separation efficiency of the membranes and are presented here.

## 2. EXPERIMENTAL

### 2.1. Materials

Chitosan (*N*-deacetylation degree 84%) was obtained from Sigma-Aldrich Chemicals, USA.

Isopropanol, hydrochloric acid and glutaraldehyde were purchased from s.d. fine Chemicals Ltd., Mumbai, India. 13X zeolite was kindly supplied by M/S Zeolite and Allied products Pvt. Ltd., Mumbai. All the chemicals were of reagent grade and used without further purification. Deionized water generated by RO system was used throughout the research work.

### 2.2. Membrane Preparation

2 wt. % solution of CS in 2% (v/v) aqueous acetic acid mixture was prepared by stirring for about 24 h at room temperature. The solution was then filtered to separate any undissolved matter and obtained the bubble-free solution. The resulting homogeneous solution was spread onto a glass plate with the aid of a casting knife in a dust-free atmosphere at room temperature. After being dried for about 48 h, the membrane was subsequently peeled-off.

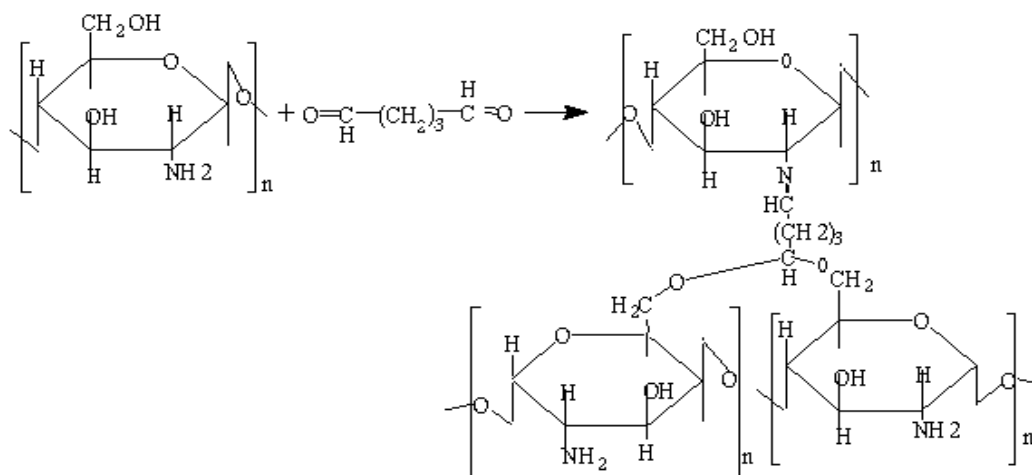
To prepare zeolite-incorporated chitosan membranes, a known amount of 13X zeolite was added into the chitosan solution. The amount of chitosan was kept constant for each membrane. The mixed solution was stirred for about 24 h and then, it was kept in an ultrasonic bath for about 30 min to break the aggregated crystals of zeolite and so as to improve the dispersion of zeolite in the polymer matrix. It was then filtered and left overnight to get a homogeneous solution. The resulting solution was poured onto a glass plate and the membrane was dried as mentioned above. The prepared membranes were then crosslinked in a bath containing with, 84 vol. % isopropanol, 10 vol. % water, 5 vol. % of glutaraldehyde, as the crosslinker and 1 vol. % hydrochloric acid, as the catalyst for a period of 2 hours. The amount of 13X zeolite with respect to CS varied as 0, 10, 20 and 30 mass%, and the membranes thus obtained were designated as CS-0, CS-10, CS-20 and CS-30 respectively. The schematic representation of CS crosslinked with glutaraldehyde is shown in Scheme.1.

### 2.3. Membrane Characterization

All the prepared membranes used in the present pervaporation measurements were characterized using the methods described below:

### 2.4. Fourier Transform Infrared (FTIR) Spectroscopic Studies

Pure CS, crosslinked CS and 13X zeolite incorporated CS membranes were scanned equipped using FTIR spectrometer (Bomem MB: 3000, Canada), equipped with attenuated total reflectance (ATR). Dry membranes were characterized in the range of 4000-500  $\text{cm}^{-1}$  at a scan rate of 25  $\text{cm}^{-1}$  under  $\text{N}_2$  atmosphere.



**Scheme. 1:** Reaction scheme of chitosan cross linked with glutaraldehyde.

### 2.5. X-Ray Diffraction (XRD) Analysis

A Siemens D 5000 (Germany) X-ray diffractometer was used to study the solid-state morphology of CS-0 and CS-20 membrane. X-rays of 1.5406 Å wavelength was generated by a Cu-K $\alpha$  source for this study. The angles of diffractions were varied from 2 $^{\circ}$  to 65 $^{\circ}$  in order to identify any changes in the crystal structure and intermolecular distances between intersegmental chains after modification.

### 2.6. Scanning Electron Micrograph (SEM) Studies

Scanning electron micrographs (SEM) of surface and cross-section were taken for the unfilled CS membrane and zeolite filled CS membranes, using software controlled digital scanning electron microscope–JEOL JSM 5410, Japan.

### 2.7. Thermogravimetric Analysis (TGA)

Thermal stability of the polymer films was examined using TG instruments (Model: SDT Q600, U.K) in the temperature range of 25-600  $^{\circ}$ C at a heating rate of 10  $^{\circ}$ C/min, with nitrogen flushed at 100 ml/min. The samples were subjected to TGA both before and after incorporation of zeolite to determine the thermal stability and decomposition characteristics.

### 2.8. Differential Scanning Calorimetry (DSC) Studies

DSC curves of the polymer films was examined using TG instruments (Model: SDT Q600, U.K) in the temperature range of 25-600  $^{\circ}$ C at a heating rate of 10  $^{\circ}$ C/min, with nitrogen flushed at 100 ml/min. The samples were subjected to DSC for both before and after incorporation of zeolite to determine the thermal stability and decomposition characteristics.

### 2.9. Mechanical Properties Studies

Tensile strength experiments were performed at room temperature using an Instron-type tensile testing machine (Shimadzu make and AGS-10 kN model) with an operating head load of 5kN and

keeping speed of testing was set at the rate of 12.5 mm/min. Cross-sectional area of the sample of known width and thickness was calculated. Tensile strength was calculated using the equation.

$$\text{Tensile strength} = \frac{\text{Max load}}{\text{Cross sectional area}} \quad (1)$$

(N/mm $^2$ )

### 2.10. Pervaporation Experiments

The equipment used to perform the PV experiments remained the same as described earlier Sudhakar et al. [25-26]. The pervaporation cell consisted of two bell-shaped B-24 size glass column reducers/couplers clamped together with external padded flanges by means of tie rods to give a vacuum tight arrangement. The top half was used as the feed chamber and the bottom one worked as the permeate chamber. The membrane was supported by a stainless steel porous plate which was embedded with a mesh of the same material to provide a smooth uniform surface. Teflon gaskets were fixed by means of high vacuum silicone grease on either side of the membrane and the sandwich was placed between the two glass column couplers and secured tightly. The effective membrane area that was in contact with feed was 20 cm $^2$ . After fixing the membrane, the cell was installed in the manifold and connected to the permeate line by means of a B-24 glass cone which was fixed on one side to a high vacuum glass valve followed by a glass condenser trap which consisted of a small detachable collector. The trap was placed in a Dewar flask containing liquid nitrogen for condensing the permeate vapors. A rotary vacuum pump was used to maintain the permeate side pressure which was measured with an Edward's McLeod gauge of scale in the range 0.01-10 mmHg. High vacuum rubber tubing was used to connect the various accessories to the experimental manifold. All glass cone–socket joints were fixed with good quality high vacuum grease (Dow Corning, USA).

Initially the membrane was soaked in the feed solution overnight to attain equilibrium. During the experiments the membrane upstream side was maintained at atmospheric pressure and the downstream side pressure was controlled by adjusting the value for vacuum release (vent). The permeate was condensed in the trap for a period of 6-8 hrs and then collected in a simple bottle for evaluation of its weight to determine the flux and analyzed by gas chromatography to calculate the selectivity. Flux ( $J_i$ ) was calculated using the Eq. (2). The feed was kept in continuous stirring mode using an overhead stirring motor to minimize the concentration polarization.

$$J_i = W_i / At \quad (2)$$

Here  $W_i$  represents the mass of water in permeate (kg),  $A$  is the membrane area ( $m^2$ ) and  $t$  represents the permeation time (h).

The composition of both feed and permeate composition was determined using a Nucon gas chromatograph (Model 5765) installed with thermal conductivity detector (TCD) and packed column of 10% diethylene glycol sebacate (DEGS) on 80/100 Supelcoport of 1/8<sup>11</sup> internal diameter and 2 m length. The oven temperature was maintained at 70 °C (isothermal) while the injector and detector temperatures were maintained at 150°C each. The sample injection size was 1  $\mu$ l and pure hydrogen was used as the carrier gas at a pressure of 1 kg/cm<sup>2</sup>. The GC response was calibrated for this particular column and conditions with known compositions of IPA–water mixtures and the calibration factors were feed into the software to obtain correct analysis for unknown samples, and the errors in the pervaporation measurements were less than 1.0%. The selectivity of the 13X zeolite-filled membranes was evaluated by Eq. (3). Membrane selectivity,  $\alpha$ , is the ratio of permeability coefficient of water to that of isopropanol, which is calculated from their respective wt. concentrations in feed and permeate as given below:

$$\alpha = y(1-x)/x(1-y) \quad (3)$$

where  $y$  is the permeate weight fraction of the faster permeating component (water) and  $x$  is its feed weight fraction.

### 2.11. Sorption Experiments

Interaction of the membranes with the pure liquid components of the feed mixture was determined by gravimetric sorption experiments. Dried membranes of known weight were immersed in different IPA-water mixtures for 48 hrs. When the sample attained constant weight, the membrane

was carefully wiped off with filter papers to remove surface liquid, and then quickly weighed. Degree of swelling was calculated as:

$$\text{Degree of swelling} = M_s / M_d \quad (4)$$

where  $M_s$  is mass of the swollen membrane in (g) and  $M_d$  is mass of the dry membrane in (g). The percent sorption was calculated using the equation:

$$\% \text{ Sorption} = [(M_s - M_d) / M_d] \times 100 \quad (5)$$

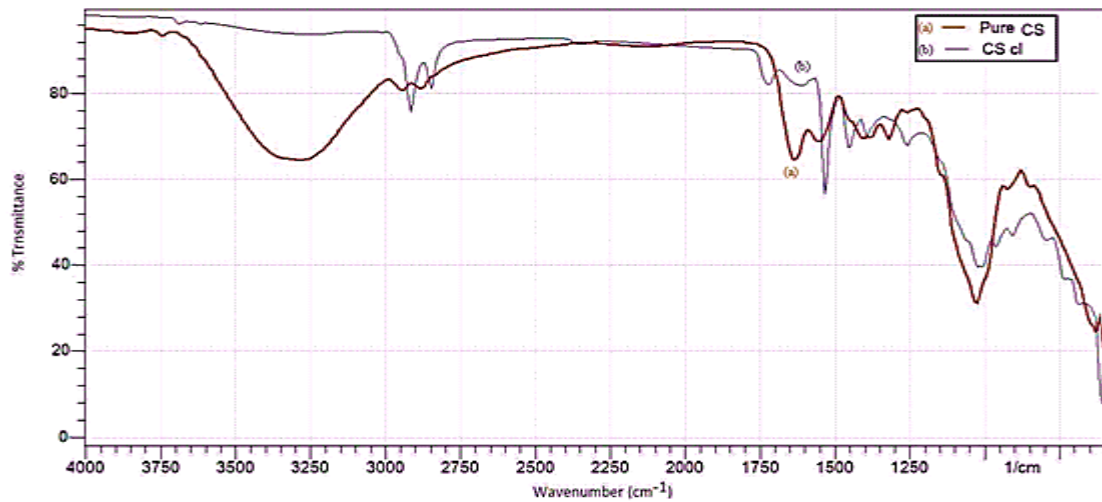
## 3. RESULTS AND DISCUSSION

### 3.1. FTIR Analysis

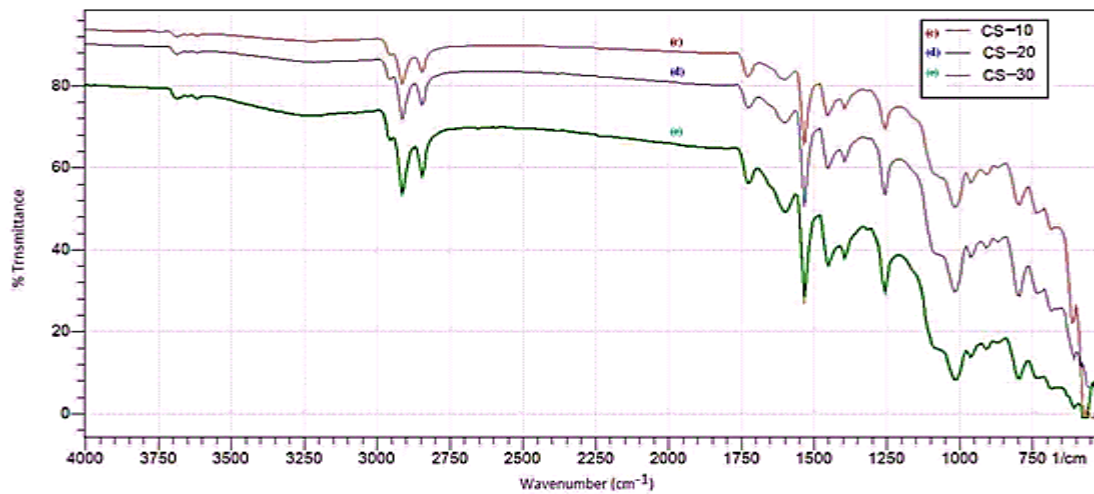
FT-IR spectra of pure CS (a), crosslinked CS (b) and zeolite filled CS membranes are shown in Figure 1 (A) and 1(B) respectively. For pure chitosan membrane, the characteristic bands at 3400  $cm^{-1}$ , 1650  $cm^{-1}$  and 1550  $cm^{-1}$  are attributed to hydroxyl group, amide I and amide II groups, respectively. The bands at 1070  $cm^{-1}$ , 1380  $cm^{-1}$  and 1160  $cm^{-1}$  are due to the C-O stretching, -CH<sub>2</sub> bending and asymmetric stretching of C-O-C [27]. IR spectra have been used to understand the crosslinking reaction with glutaraldehyde (GA). In Scheme.1, the bands at 1650 and 1560  $cm^{-1}$  represent amino I and amino II functional groups in chitosan [28-29]. The intensity of the band at 3400  $cm^{-1}$  decreases notably after zeolite modification, as a result of consumption of hydroxyl groups of zeolite by condensing with the silanol groups. In Figure 1 (B) a strong peak appeared at around 1020  $cm^{-1}$  and is assigned to C-O stretching of CS. The Si-O band [30] also appeared at the same wavelength upon zeolite loading in the polymer matrix and hence, C-O and Si-O bands are almost overlapping in the spectra.

### 3.2. X-Ray Diffraction

Figure.2 illustrates the wide angle X-ray diffraction (WAXD) patterns of chitosan (2.a) and zeolite incorporated chitosan membrane (2.b). These diffractograms indicates the semi crystallinity of chitosan crystallinity of CS-zeolite membrane. Pure CS membrane exhibited two characteristic peaks at  $2\theta = 13^\circ$ . For polymer-zeolite mixed matrix membrane, the presence of zeolite particles interfered the ordered packing of CS chains, and leads to the hydrogen bonding interactions between CS and zeolite [31]. The CS/zeolite film showed characteristic peaks of both components and the differences may be justified by the incorporation of zeolite crystals in the chitosan film membranes, which intern confirmed the more semi crystalline nature of the CS-zeolite membrane.



(A)



(B)

**Figure 1.** (A) FTIR spectra (a) Pure CS and (b) cross linked CS; (B) Zeolite filled crosslinked membranes (c) CS-10; (d) CS-20; and (e) CS-30.

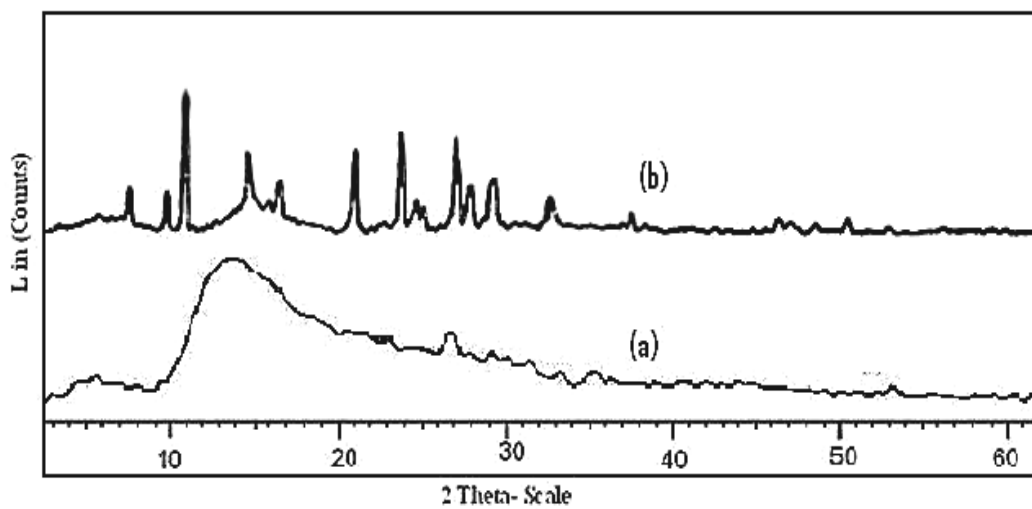


**Figure 2.** Wide angle X-ray diffraction patterns of Zeolite filled chitosan membranes: (a) CS-0; and (b) CS-20.

### 3.3. SEM Analysis

Figure 3(A) shows the scanning electron micrographs of pure chitosan and zeolite filled CS membranes. No appreciable pore and phase separation between CS and zeolite could be observed, indicating the defect-free dense membrane. In addition zeolite was quite uniformly distributed in the membrane. Figure 3(B) presents the cross-section SEM images of chitosan and zeolite filled CS membranes. While pure chitosan membrane Figure 3(B)(e) shows a void-free dense structure, voids around the modified zeolite particles can be clearly observed in the zeolite filled CS membranes. Much better interfacial morphology was obtained after zeolite incorporation as shown in Figure 3(B), confirming an improvement in compatibility between the polymer and inorganic filler. It should be mentioned that, the membrane displays better interfacial morphology CS-13X zeolite membranes. Hence, it is better to have a uniform distribution of 13X zeolite filled CS membranes with exhibit enhance flux and selectivity.

### 3.4. TGA Studies

Figure 4 represents TGA curves for chitosan and zeolite filled membranes. The thermograms for all samples showed similar trends. These curves shows the thermal stability of the CS and CS-zeolite filled membranes, for all membranes two major weight loss peaks were observed the first peak (100-110 °C) comes to loss of water. The second peak (180-320 °C) corresponds to the degradation of the sample. In general, both the intermolecular and the intramolecular hydrogen bonds could make contributions to enhancing the thermal stability of the membrane [32]. When incorporating 13X zeolite strong hydrogen bonding interactions between CS and zeolite were formed which could dramatically suppress the decomposition of CS chains, and the CS/zeo membrane exhibited better thermal stability than pure CS membrane [Figure. 4. a].

### 3.5. DSC Studies

DSC thermograms of CS and zeolite filled CS membranes shown in Figure 5. The cross linked CS (a) showed a typical DSC thermogram where it is believed to result from the change in the crystalline morphology of zeolite filled CS membrane. It was of particular interest to estimate how the thermal transition in CS varied with zeolite. The homogeneous nature of CS and zeolite incorporated CS membranes represented by curves (a-d) gave relatively sharp melting endotherms with a melting temperature peak ( $T_m$ ) observed around 220°C. However, upon introducing zeolite, increase in endothermic peak was observed. This result indicates that CS-zeolite membranes are more stable at high temperatures than the unfilled CS,

that is zeolite incorporated Cs membranes are more thermally stable.

### 3.6. Mechanical Properties

Incorporation of 13X zeolite into chitosan improved the tensile strength of the membranes. Chitosan (CS-0) and zeolite incorporated chitosan membranes (CS-10, CS-20 and CS-30) exhibited tensile strengths of 6.07, 9.53, 12.11 and 14.60 N/mm<sup>2</sup> respectively. The results indicate that with increase in zeolite content in CS the tensile strength increases. Extensive intra and intermolecular hydrogen bond interactions involving -NH<sub>2</sub> and -OH groups of CS besides the formation of an interpenetrating polymer network upon crosslinking are responsible for such as increase in mechanical strength.

### 3.7. Membrane Sorption Properties

The variation of degree of sorption vs percentage of water through CS and zeolite filled CS membranes are shown in Figure 6. It is noticed from this figure that as the water concentration in the feed increased the percent sorption increased as shown in the following order CS-30 > CS-20 > CS-10 > CS-0.

### 3.8. Pervaporation Properties

The variation of flux and selectivity with wt. % of water in the feed for CS and zeolite filled CS membranes are shown in Figure 7(A) and 7(B) respectively. The effect of zeolite loading between 0-30 wt.% in CS was tested, since addition of zeolite give varying flux and selectivity data for the zeolite incorporated CS membranes. Now the improvement of membrane performance shown by zeolite filled membranes over that of pure CS membrane is due to filler-polymer and membrane-solvent interactions. The effect of zeolite content of CS matrix was studied for feed containing 0-40 wt. % of water and with increasing loading of 13X zeolites. From the results it is noticed that both flux and selectivity were increased, which can be attributed to the hydrophilic nature of 13X zeolite because it adsorbs large quantities of water through molecular size pores. To thereby creating free channels for transporting water molecules through the membranes. It can be also expected that hydrophilic-hydrophilic interactions would reject organic (IPA) component of the feed but allows only water molecules.

A strong interaction between hydrophilic 13X zeolite and water molecules would allow water to transport across the membrane but at high loading (30 wt. %) of 13X zeolite in CS leads to flux of 0.125 kg/m<sup>2</sup>h for IPA-water are observed.

At lower loading of 13X zeolite particles as well as with unfilled CS membrane, both selectivity and

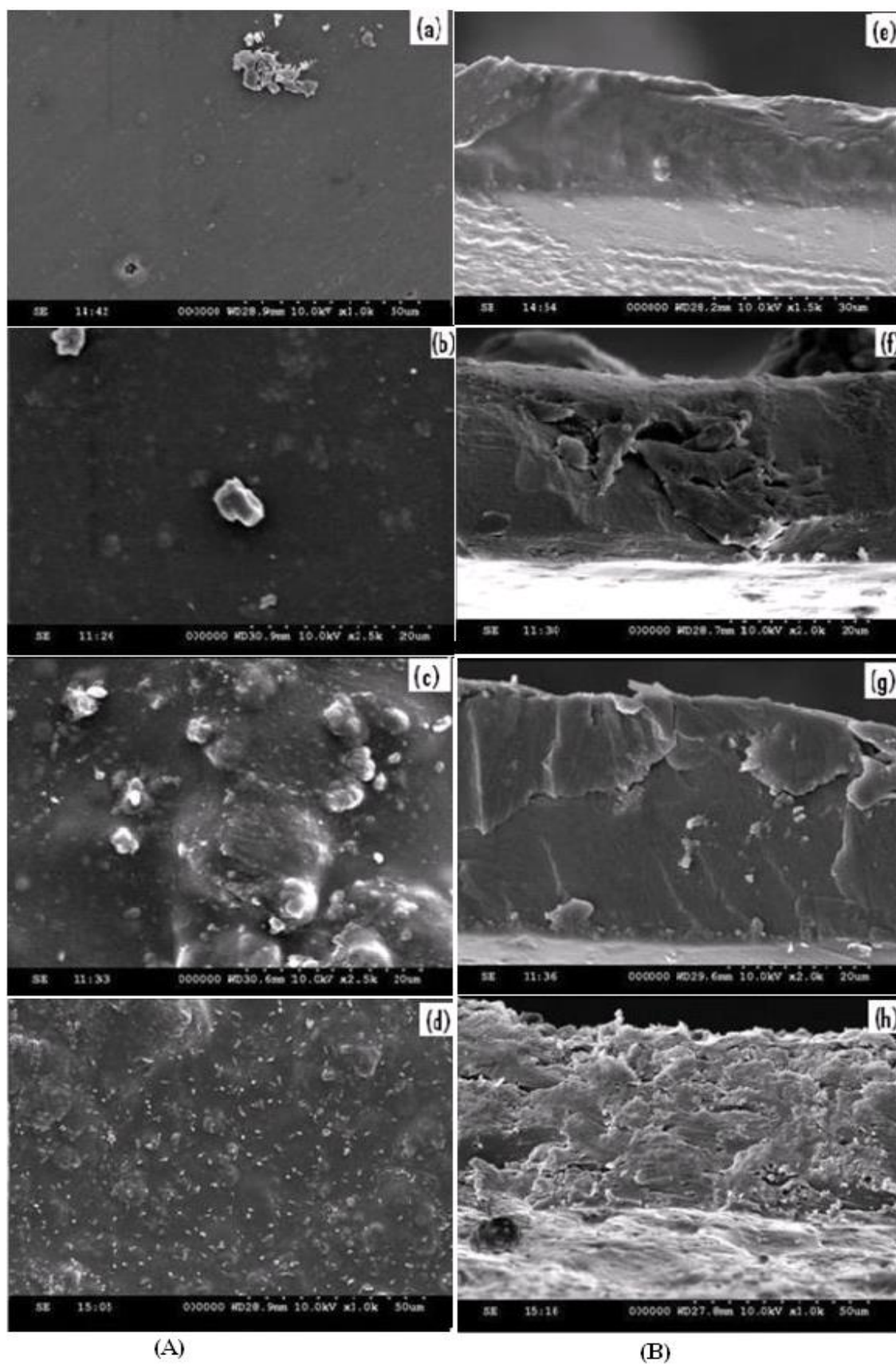


**Figure 3.** (A) SEM pictures Surfaces of the: (a) CS-0; (b) CS-10; (c) CS-20; and (d) CS-30. (B) Cross section of the: (e) CS-0; (f) CS-10; (g) CS-20; (h) CS-30.

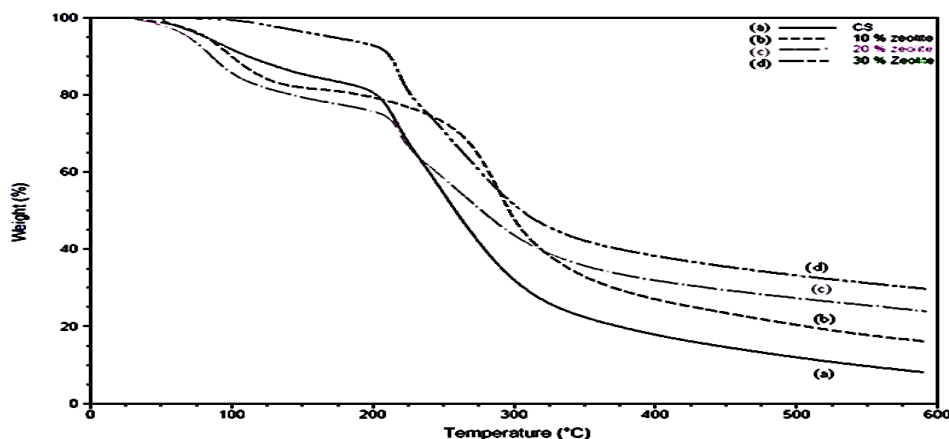


Figure 4. TGA analysis of (a) CS-0; (b) CS-10; (c) CS-20; (d) CS-30.

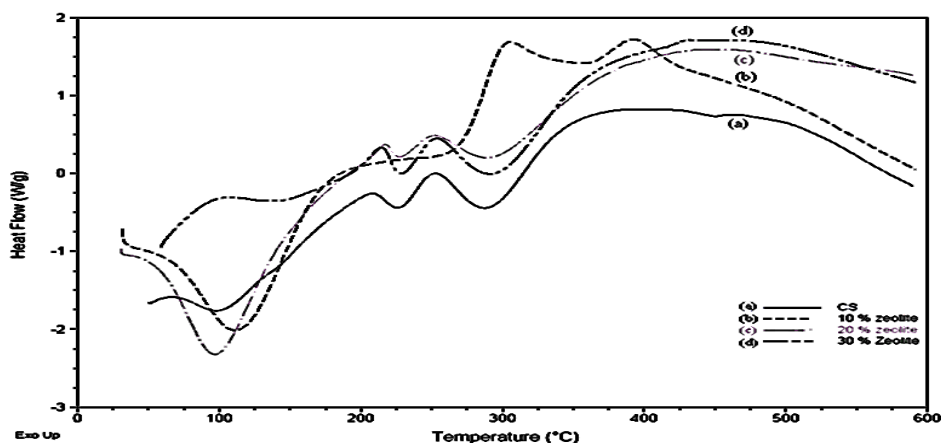


Figure 5. DSC curves of (a) CS-0; (b) CS-10; (c) CS-20; (d) CS-30

flux values are lower. On the other hand zeolite incorporated CS membranes have higher PV performances than CS-0 membrane thus; it would extract more amount of water compared with organic molecules. By careful observation it is noticed that zeolite incorporated membranes have better PV performances due to the following: (i) adsorption and diffusion of water molecules through the pores of 13X zeolite and (ii) transport along the boundaries between the molecular sieve crystals and the CS matrix. The former process is more dominant than the latter, since zeolite incorporated membranes would possess good interface contact, whereas in the latter, this contact may be less dominant, if zeolite 13X-polymer interface is poor Chon et al [33]. At any rate, the unique properties like molecular sieving effect and adsorption preference are important if 13X zeolite particles are compatible with CS matrix. In addition, interfacial interactions between 13X zeolite and polymer are also critical to the optimum performance to the separation. Thus, 13X zeolite particles could discriminate components of the aqueous-organic mixtures either by exclusion of competing molecules on the basis of molecular size and shape or by adsorption preference; hence, by incorporating 13x zeolite particles, it is expected to enhance the separation performance of CS. 13X

zeolite has a pore size of (0.9 nm), which is larger than the kinetic diameter of water (0.296 nm), IPA (0.43 nm). Comparatively, water molecule size is smaller to IPA molecule, beside this it can also be attributed that smaller size water molecules may diffuse faster than IPA molecules. This leads to the increase values of selectivity with increasing zeolite loading for the feed as shown in Figure 7. Thus, viewed from any angle, i.e., either through polymer solvent or through polymer-zeolite interactions, as well as based on size exclusion effect, it is obvious that incorporation of 13X zeolite into CS would boost the PV performance over that of plain CS membrane. Even on the basis of sorption and diffusion principles also, the separation efficiency of membranes is higher for water than organics. Sorption is usually favored by specific type of hydrophilic-hydrophilic interactions, whereas diffusion is affected by membrane morphology in addition to chain mobility. The improvement in selectivity and flux data of incorporating zeolite membranes is influenced by 13X zeolite in CS.

Flux for unfilled CS membrane is lower than incorporating zeolite membranes for the studied feed compositions. For instance, this is indicative of the fact that liquid-liquid interactions might vary



depending upon the nature of the membrane. In addition, plasticization of membrane polymer in the presence of different media and chain mobility would also influence membrane performance. Such an effect would be more favorable for water transport than organics, because water will occupy free channels created within incorporating zeolite membranes and thus, the recovery of water will be more on permeate side. In the feed mixtures, flux increased systematically with increasing loadings of 13X zeolite. The minimum value of flux observed for 10 wt. % 13X zeolite loaded CS membrane is due to lesser surface diffusion and activated transport of water through the pores of incorporating zeolite membranes, but at 30 wt. % 13X zeolite loading, adsorption capacity of zeolite particles would increase due to increased hydrophilicity of zeolite membranes, thereby offering higher permeation flux.

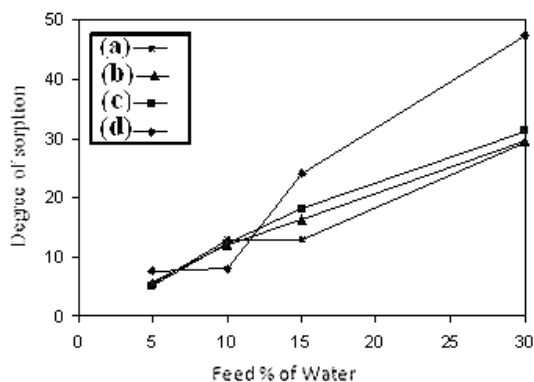


**Figure 6.** Plots of Degree of sorption vs Percentage of water (a) CS-0; (b) CS-10; (c) CS-20 and (d) CS-30 incorporated zeolite crosslinked membranes

Figure 7 illustrates the relationship between membrane performance and water composition for IPA-water mixtures in case of unfilled CS and 30 wt. % 13X zeolite-loaded CS at 30°C. Flux increases with increasing water content of the feed, which is caused by higher concentration of water in the membrane, but selectivity decreased for the feed.

#### 4. CONCLUSIONS

In the present work, chitosan-13X zeolite composite membranes were successfully prepared. The suitable conditions for uniformly disperse the zeolite in chitosan solution were found, with which composite membranes with homogeneously dispersed zeolites in chitosan could be fabricated. The pervaporation performance of the composite membranes is comparable to that of commercial membranes, suggesting that the membranes have potential for commercialization.

**Acknowledgements:** Authors thank UGC New Delhi for providing financial assistance to one of

the authors (H. Sudhakar) under UGC-RGNF scheme Ltr No: F.16-89/2006(SA-II) and No. F./PDFSS-2012-13-SC-AND-2486.

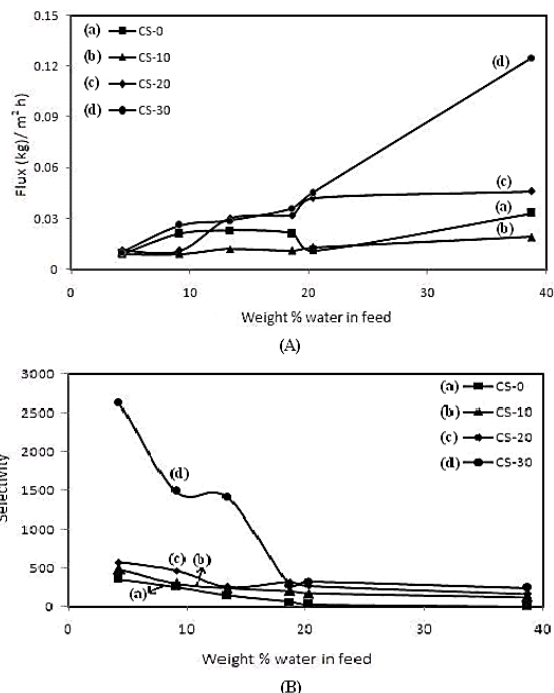


**Figure 7.**(A) Plots of water flux vs weight % water in feed; (B) Plots of selectivity vs weight % water in feed CS and 13X zeolite incorporated CS membranes.

#### 5. REFERENCES

- [1]. T. Uragami, K.Okazaki, H.Matsugi, T.Miyata (2002) Structure and Permeation Characteristics of an Aqueous Ethanol Solution of Organic-Inorganic Hybrid Membranes Composed of Poly (vinyl alcohol) and Tetraethoxysilane, *Macromolecules*, **35(24)**: 9156-9163.
- [2]. V.A.Tuan, S. Li, J.LFalconer, R.D. Noble (2002) Separating organics from water by pervaporation with isomorphously-substituted MFI zeolite, *Journal of Membrane Science*, **196**: 111-123.
- [3]. J.Neel, (1994) *Introduction to Pervaporation*, Elsevier: Amsterdam, The Netherlands.
- [4]. A.A. Kittur, M.Y.Kariduraganavar, U.S.Toti, K.Ramesh, T.M.Aminabhavi (2003) Pervaporation separation of water-isopropanol mixtures using ZSM-5 zeolite incorporated poly (vinyl alcohol) membranes, *Journal of Applied Polymer Science*, **90**: 2441-2448.
- [5]. D.Sarkhel, D.Roy, M. Bandyopadhyay, P. Bhattacharya (2003) Studies on separation characteristics and pseudo-equilibrium relationship in pervaporation of benzene-cyclohexane mixtures through composite PVA membranes on PAN supports, *Separation and Purification Technology*, **30**: 89-96.

- [6]. S.C. George, K.N. Ninan, S. Thomas (2000) Pervaporation separation of chlorinated hydrocarbon and acetone mixtures with crosslinked styrene-butadiene rubber and natural rubber blend membranes, *Journal of Membrane Science*, **176**: 131-142.
- [7]. S.P. Kusumocahyo, M. Sudoh (1999) Dehydration of acetic acid by pervaporation with charged membranes, *Journal of Membrane Science*, **161**:77-83.
- [8]. A.A. Kittur, S.S. Kulkarni, M.I. Aralaguppi, M.Y. Kariduraganavar (2005) Preparation and characterization of novel pervaporation membranes for the separation of water-isopropanol mixtures using chitosan and NaY zeolite, *Journal of Membrane Science*, **247**:75-86.
- [9]. X.Lin, E. Kikuchi, M. Matsukata, (2000) Preparation of mordenite membranes on  $\alpha$ -alumina tubular supports for pervaporation of water-isopropyl alcohol mixtures, *Chemical Communications*, 957-958.
- [10]. R.Y.M. Haung, R. Pal, G.Y. Moon (1999) Crosslinked chitosan composite membrane for the pervaporation dehydration of alcohol mixtures and enhancement of structural stability of chitosan/polysulfone membranes, *Journal of Membrane Science*, **160**: 17-30
- [11]. X.Feng, R.Y.M. Haung (1997) Liquid Separation by Membrane Pervaporation: A Review, *Industrial Engineering Chemistry Research*, **36** (4): 1048-1066.
- [12]. S.Y. Nam, H.J. Chun, Y.M. Lee (1999) Pervaporation separation of water-isopropanol mixture using carboxymethylated poly (vinyl alcohol) composite membranes, *Journal of Applied Polymer Science*, **72**: 241-249.
- [13]. G.Y. Moon, R. Pal, R.Y.M. Haung (1999) Novel two-ply composite membranes of chitosan and sodium alginate for the pervaporation dehydration of isopropanol and ethanol, *Journal of Membrane Science*, **156**:17-27.
- [14]. S.S. Kulkarni, A.A. Kittur, M.I. Aralaguppi, M.Y. Kariduraganavar (2004) Synthesis and characterization of hybrid membranes using poly(vinyl alcohol) and tetraethylorthosilicate for the pervaporation separation of water-isopropanol mixtures *Journal of Applied Polymer Science*, **94**: 1304-1315.
- [15]. M.D. Kurkuri, U.S. Toti, T.M. Aminabhavi (2002) Syntheses and characterization of blend membranes of sodium alginate and poly (vinyl alcohol) for the pervaporation separation of water + isopropanol mixtures, *Journal of Applied Polymer Science*, **86**: 3642-3651.
- [16]. K.C. Santosh, A.A. Kittur, S.S. Kulkarni, Y.K. Mahadevappa (2007) Development of novel blocked diisocyanate crosslinked chitosan membranes for pervaporation separation of water-isopropanol mixtures, *Journal of Membrane Science*, **302**: 197-206.
- [17]. K.C. Santosh, Y.K. Mahadevappa (2009) Development of novel composite membranes using quaternized chitosan and Na<sup>+</sup>-MMT clay for the pervaporation dehydration of Isopropanol, *Journal of Colloid and Interface Science*, **338**: 111-120.
- [18]. Zheng Cui, Y. Xiang, J.Si, M. Yang , Qi Zhang, Tao Zhang, (2008) Ionic interactions between sulfuric acid and chitosan membranes, *Carbohydrate Polymers*, **73**(1):111-116.
- [19]. X. Chen, H.Yang, Z. Gu, Z. Shao (2001) Preparation and characterization of HY zeolite-filled chitosan membranes for pervaporation separation, *Journal of Applied Polymer Science*, **79**:1144-1149.
- [20]. M. Jia, K.V. Peinemann, R.D. Behling (1991) Molecular sieving effect of the zeolite-filled silicone rubber membranes in gas permeation, *Journal of Membrane Science*, **57**: 289-292.
- [21]. M. Ghazali Hj, M. Nawawi, LeT Ngoc Tram (2004) Pervaporation dehydration of isopropanol-water mixtures using chitosan zeolite- as membranes, *Journal of Teknologi*, **41**(F): 61-72.
- [22]. Laura Casado, Reyes Mallada, Carlos Téllez, Joaquín Coronas, Miguel Menéndez, Jesús Santamaria (2003) Preparation, characterization and pervaporation performance of mordenite membranes, *Journal of Membrane Science*, **216**: 135-147.
- [23]. Shin-Ling Wee, Ching-Thian Tye, Subhash Bhatia (2008) Membrane separation process- Pervaporation through zeolite membrane *Separation and Purification Technology*, **63**: 500-516.
- [24]. Xin Chen, Hu Yang, Zhengyu Gu, Zhengzhong Shao (2001) Preparation and Characterization of HY Zeolite-Filled Chitosan Membranes for Pervaporation Separation, *Journal of Applied Polymer Science*, **79**: 1144-1149.
- [25]. H.Sudhakar, K. Chowdoji Rao, S. Sridhar (2010) Effect of Multi-walled Carbon Nanotubes on Pervaporation Characteristics of Chitosan Membrane, *Designed Monomers and Polymers*, **13**: 287-299.
- [26]. H. Sudhakar, C. Venkata Prasad, K. Sunitha, K. Chowdoji Rao, M.C.S. Subha, S. Sridhar (2011) Pervaporation separation of IPA-water mixtures through 4A zeolite-filled sodium alginate membranes, *Journal of Applied Polymer Science*, **121** (5): 2717.
- [27]. P. Kanti, K. Srigowri, J. Madhuri, B. Smitha, S. Sridhar (2004) Dehydration of ethanol

- through blend membranes of chitosan and sodium alginate by pervaporation, *Separation and Purification Technology*, **40**: 259-266.
- [28]. N.J. Bellamy (1975) *The Infrared Spectra of Complex Molecules*, Chapman & Hall, London.
- [29]. G.O. Aspinall (1982) *Spectroscopic Method in the Polysaccharides*, vol. 1, Academic Press: New York (Chapter 4).
- [30]. V. Chavasit, C. Kienzle-Sterzer, J.A. Torres (1988) Formation and characterization of an insoluble polyelectrolyte complex: Chitosan-polyacrylic acid, *Polymer Bulletin*, **19**: 223-230.
- [31]. W. Yuan, W. Hong, Z. Bin, Z. Hong, Z. Jiang, X. Hao, B. Wang (2007) Sorbitol-plasticized chitosan/zeolite hybrid membrane for direct methanol fuel cell, *Journal of Power Sources*, **172**: 604-612.
- [32]. Y. Wan, K.A.M. Creber, B. Peppley, V.T. Bui (2006) Chitosan-based solid electrolyte composite membranes: I. Preparation and characterization *J. Membr. Sci.*, **280**: 666-674.
- [33]. H. Chon, Seong IhI Woo S.E. Park (1996) *Recent Advances and New Horizons in Zeolite Science and Technology*, Elsevier: Amsterdam, Chapter 1.